united nations
educational, scientific
and cultural
organization

international atomic
energy agency

the
abdus salam
international centre for theoretical physics

SMR/1108 - 24

COURSE ON "MEDITERRANEAN SEA(S) CIRCULATION & ECOSYSTEM FUNCTIONING"

2 - 20 November 1998

Trieste, Italy

* * *

"Three Dimensional Oligotrophic Ecosystem Models"

G. CRISPI
Osservatorio Geofisico Sperimentale
Trieste, Italy

in press
ENSO 995

ELSEVIER

Environmental Modelling & Software ●● (1998) 000–000

Environmental
Modelling & Software

Three-dimensional oligotrophic ecosystem models driven by physical forcing: the Mediterranean Sea case

G. Crispi *, A. Crise, C. Solidoro

Osservatorio Geofisico Sperimentale, P.O. Box 2011, 34016 Trieste, Italy

Received ??/??/??; received in revised form ??/??/??; accepted ??/??/??

Abstract

An analysis of existing biochemical datasets, collected using different measurements methods, confirms peculiarities of the Mediterranean Sea, such as its oligotrophy, easterly decreasing gradients, and influence of hydrodynamics on the biochemical patterns. Thus assessment of this marine environment requires a model based on a three-dimensional characterization of the ecosystem dynamics. The model, which covers all the Mediterranean basin, conceptually takes into accounts the cycles of nitrogen and phosphorus through the detritus and food chains. It includes as major compartments dissolved inorganic nutrients, two pools of phytoplankton producers, one of zooplankton, and detritus. Dynamic of dissolved oxygen is also simulated. Simulations are presented and results from this conceptualization are reported. © 1998 Elsevier Science Ltd. All rights reserved.

Keywords: Marine ecosystems; Chemical data; Aggregated models; Mediterranean Sea

1. Introduction

Chemical data used here for analysis of major features in the Mediterranean Sea are historical and recent data. The historical data are: NODC dataset (Levitus et al., 1993; Conkright et al., 1994) from 1948 to 1973 for the Eastern Mediterranean Sea and ABCD dataset (Zavatarelli et al., 1998), periods 1911–14 and 1948–91 for the Adriatic Sea. The recent data come from cruises in different areas: MEDIPROD I (Coste et al., 1972) and DISCOVERY (Cruzado, 1995) in the Western Mediterranean Sea, and POEM (Rabitti et al., 1994) in the Eastern Mediterranean Sea.

This dataset exhibits the following peculiarities regarding nutrients:

1. an extreme oligotrophy with respect to the world ocean;
2. a huge spatial variability with maxima in coastal areas, due to rivers run-off and/or anthropic pressure;
3. significant seasonal excursion with variances of the same order as the mean values.

The first peculiarity is a direct consequence of concentration characteristic of the Mediterranean. The inverse estuarine circulation of the whole basin creates a negative budget for the nutrients at the Gibraltar Strait (Coste et al., 1988), importing nutrient poor surface water from the Atlantic Ocean and exporting into it relatively nutrient rich intermediate water.

Permanent and recurrent gyres, mainly cyclonic in the northern area of the basin and anticyclonic in the southern one, determine the regional distributions that affect the vertical advection of nutrients, which is the determining factor for new production (Dugdale and Wilkerson, 1988).

Moreover, processes at a scale smaller than the abovementioned sub-basin scale, such as fronts, coastal upwellings and transient gyres, can determine a few kilometers coherence in the ecosystem function, as well as shorter temporal variabilities in the biochemical processes (Margalef, 1985).

Thus an analysis of the Mediterranean ecosystem variability must take into account the detailed hydrodynamics of the basin, which can be done by coupling the biochemical processes with a 3-D model of the entire basin.

Primary production in the Mediterranean ecosystem is limited both by the nutrient availability, distributed by

---

* Corresponding author. Tel.: + 40-2140205; Fax: + 40-327307; E-mail: gcrispi@ogs.trieste.it

1364-8152/98/$19.00 © 1998 Elsevier Science Ltd. All rights reserved.
PII: S1364-8152(98)00054-1

Author's

oceanographic processes present at different time and space scale, and by irradiance and its penetration in the water column.

To obtain the temporal and spatial evolution of the lower trophic levels, the biological processes are conceptualized in a highly aggregated scheme. The rationale is that any model is a simplification of the real processes whose full complexity is beyond our capability to mimic. Therefore the aim of this model is not only to follow the evolution of the biogeochemical compartments chosen in the aggregated description, but also ~~possibly~~ to understand major features of ecosystem function and to learn something about processes and the large scale ecological responses of the ecosystem to different scenarios of environmental conditions.

In order to cope with the huge variability of a basin as large and differentiated as the Mediterranean one, two different groups of primary producers are considered, the first being representative of the small autotrophic microflagellates, the picoplankton, and the second of the large diatoms, the netplankton. Both groups, each one at its own specific rate, are grazed by zooplankton, and their growth depends on temperature, irradiance and nutrient availability. The potentially limiting nutrients taken into account in the model are inorganic nitrogen, both in oxidized and reduced form, and reactive phosphorus. Silicate is not taken into account because experimental data suggest that this element is not generally a limiting factor.

As indicated in Fig. 1, depicting the major steps of the cycles of macronutrients, the model can be aggregated further, by the aggregation of functionally similar state variables, up to a representation taking into account a nutrient N, a single planktonic pool P, and a detritus compartment, D.

While this aggregated NPD variant has been directly implemented in the 3-D structure of the model, the one including all ten variables has been tested on a 1-D vertical model, before coupling it with the basin scale model.

In the next section the primitive equation model is described, which accounts for the hydrodynamical variables, velocities and temperature, to be coupled with the ecological model. Afterwards the ten variables model is discussed and a 1-D application is shown. In the last session the coupling is discussed taking into account a nitrate-based model, giving also some perspectives into the applications of such a model.

2. Primitive equation model

The hydrodynamics are based on the following fully 3-D primitive equations in a spherical coordinate system (λ,φ,z) using the following assumptions: the Boussinesq, the hydrostatic and the rigid-lid approximations.

$$\frac{\partial \vec{v}}{\partial t} + (\vec{u} \cdot \nabla)\vec{v} + \vec{f} \times \vec{v} = -\frac{1}{\rho_0}\nabla_H p - A_H \nabla_H^4 \vec{v} + \overset{Av}{a_v} \frac{\partial^2 \vec{v}}{\partial z^2} \qquad (1)$$

← Av

$$\frac{\partial p}{\partial z} = -\rho g \qquad (2)$$

$$\nabla \cdot \vec{u} = 0 \qquad (3)$$

$$\frac{\partial T}{\partial t} + (\vec{u} \cdot \nabla)T = -K_H \nabla_H^4 T + K_V \frac{\partial^2 T}{\partial z^2} \qquad (4)$$

$$\frac{\partial S}{\partial t} + (\vec{u} \cdot \nabla)S = -K_H \nabla_H^4 S + K_V \frac{\partial^2 S}{\partial z^2} \qquad (5)$$

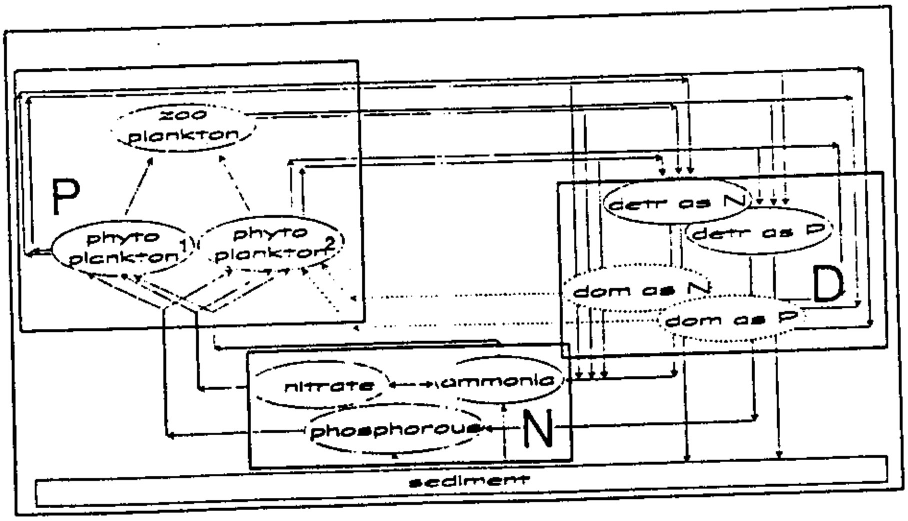

Fig. 1. Schematics of the links among the state variables. The variables of the NPD model are represented in the great boxes.

$$\rho = \rho(T,S,p) \tag{6}$$

In the preceding equations $\vec{v} = (v_\lambda, v_\varphi)$ and $w = v_z$ are respectively the horizontal and vertical components of the velocity $\vec{u}$; T and S are the temperature and salinity, while p and ρ represent the pressure and density.

The Coriolis parameter is given by $\vec{f} = 2\Omega\sin\varphi\vec{k}$ and g is the gravity constant. A_H and A_V are the horizontal and vertical constant eddy viscosity coefficients, while K_H and K_V are the horizontal and vertical constant turbulent diffusion coefficients.

The model is integrated throughout all the Mediterranean basin, with a horizontal spatial discretization of 1/4 degree and with a vertical resolution of 31 levels. On the same grid the equations describing nitrogen and phosphorus uptake, and also grazing and remineralization processes, are integrated.

For a generic biological tracer, BT, the equation is:

+

$$\frac{\partial \mathrm{BT}}{\partial t} \ominus (\overline{u} \cdot \nabla)\mathrm{BT} = -K_H \nabla_H^4 \mathrm{BT} + K_V \frac{\partial^2 \mathrm{BT}}{\partial z^2} - w_{\mathrm{BT}} \frac{\partial \mathrm{BT}}{\partial z} + \left.\frac{\partial \mathrm{BT}}{\partial t}\right|_{\mathrm{source}} \tag{7}$$

where the term $\left.\frac{\partial \mathrm{BT}}{\partial t}\right|_{\mathrm{source}}$ represents all the biological and chemical sources/sinks for the variable BT.

The details of the 3-D coupling and its parameterization are discussed in detail in Crise et al. (1998).

3. The nitrogen, phosphorus and carbon cycles

The 10 variables model, depicting the nitrogen, phosphorus and carbon cycles, has been tested on a 1-D water column, 100 m depth and discretized in 10 equal levels, driven by the temperature as computed by the 3-D model in the Ligurian Sea, and by the light intensity at the surface in the same site. This 1-D model has no flux boundary conditions at the surface and at the bottom. The euphotic zone initial conditions correspond to a well mixed layer for nutrients.

Growth limitation is described by Monod kinetic for the uptake of nitrates, ammonia and phosphorus and by the Steele (1962) formulation for light, whereas the effect of temperature is simulated by the Lassiter and Kearns (1974) function, in agreement with growth rate increasing exponentially up to an optimal temperature, and declining above it up to vanish at the temperature of arrest.

Grazing activity is described by a type II functional response (Holling, 1965), modified as in Fasham et al. (1990) in order to include the possibility that the herbivores graze upon both groups of primary producers.

A similar uptake approach is used for simulating primary production with a 1-D model in an oceanic environment, using in that case a rectangular hyperbolic grazing for netplankton and a first-order loss term for picoplankton (Bisset et al., 1994).

The detritus chain describes the remaining part of the biogeochemical cycles of carbon and macronutrients, that is the recycling, through mineralization, of the non-living organic matter, particulate and dissolved, produced by exogenous input, mortality processes, excretion and exudation, all set as linear processes. The introduction of the detritus compartment permits to follow the fate and the remineralization of the particulate matter at a basin and sub-basin scale below the euphotic zone, which are well known condition for balancing the world ocean new production (Eppley and Peterson, 1979).

In fact, a flow analysis approach (Michaels and Silver, 1988) suggests that even in oligotrophic environments where picoplankton dominates the primary production, netplankton is the main responsible of the sinking particulate matter. Anyway the production efficiencies to be used in the Mediterranean Sea ultimately rely on calibration of the overall model.

Fig. 1 shows dissolved organic matter and the microbial loop might be easily included in our schematization, but they are not taken into account explicitly, since they have a spatio–temporal scale much smaller than the other processes included. Light and temperature varies according to seasonal and night/day cycles, and the model also takes into account self-shading effects.

The dynamics of dissolved oxygen are also reproduced, since this variable, besides being frequently sampled, is an aggregated index of the quality of a water body.

The sources/sinks follow for N, A, P and O, which are respectively the concentrations of nitrate, ammonia, phosphorus and dissolved oxygen expressed in μmol l^{-1}.

$$\left.\frac{\partial N}{\partial t}\right|_{\mathrm{source}} = -R_{NC}\left(\mu_S f(I) g_S(T) \frac{P}{P+k_{PS}} \frac{N}{N+k_{NS}} \boxed{e^{-\psi_S A}} S - \mu_L f(I) g_L(T) \frac{P}{P+k_{PL}} \frac{N}{N+k_{NL}} \boxed{e^{-\psi_L A}} L\right) + \boxed{k_{nit}} \frac{O}{O+k_{AO}} A \tag{8}$$

$e^{-\psi_S A}$

$e^{-\psi_L A}$

$\leftarrow R_{nit}^{*}$

$$\left.\frac{\partial A}{\partial t}\right|_{\mathrm{source}} = -R_{NC}\left(\mu_S f(I) g_S(T) \frac{P}{P+k_{PL}} \frac{A}{A+k_{NL}} S\right.$$

$$- \mu_L f(I) g_L(T) \frac{P}{P + k_{PL}} \frac{A}{A + k_{AL}} L\Big) \tag{9}$$

$$- k^{*}_{nit} \frac{O}{O + k_{AO}} A + k^{*}_{decN} D_N + R_{NC}(k^{*}_{rS} S + k^{*}_{rL} L$$

$$+ k^{*}_{exz} Z) + R_{NC}\Big\{(1 - \epsilon_S) \frac{gSZ}{S + \alpha L + k} + (1$$

$$- \epsilon_L) \frac{g\alpha LZ}{S + \alpha L_k}\Big\}$$

$$\left.\frac{\partial P}{\partial t}\right|_{source} = - R_{PC}(\mu_S f\,\mathrm{lim}_S S + \mu_L f\,\mathrm{lim}_L L)$$

$$+ R_{PC}(k^{*}_{rS} S + k^{*}_{rL} L + k^{*}_{exz} Z) + R_{PC}\Big\{(1 \tag{10}$$

$$- \epsilon_S) \frac{gSZ}{S + \alpha L + k} + (1 - \epsilon_L) \frac{g\alpha LZ}{S + \alpha L + k}\Big\}$$

$$\left.\frac{\partial O}{\partial t}\right|_{source} = R_{OC}(\mu_S f\,\mathrm{lim}_S S + \mu_L R_{OC} f\,\mathrm{lim}_L L)$$

$$- R_{nit} k^{*}_{nit} \frac{O}{O + k_{AO}} A - R_{OC} k^{*}_{decC} D_C - R_{OC}(k^{*}_{rS} S \tag{11}$$

$$+ k^{*}_{rL} L)$$

S and L are respectively the concentrations of picoplankton and netplankton expressed in μmolC l^{-1}. Z is the concentration of the zooplankton variable in the same units.

$$\left.\frac{\partial S}{\partial t}\right|_{source} = \mu_S f\,\mathrm{lim}_S S - d_S S - k^{*}_{rS} S \tag{12}$$

$$- g \frac{SZ}{S + \alpha L + k}$$

$$\left.\frac{\partial L}{\partial t}\right|_{source} = \mu_L f\,\mathrm{lim}_L L - d_L L - k^{*}_{rL} L \tag{13}$$

$$- g \frac{\alpha LZ}{S + \alpha L + k}$$

$$\left.\frac{\partial Z}{\partial t}\right|_{source} = - d_Z Z - k^{*}_{exz} Z + g \frac{\epsilon_S S + \epsilon_L \alpha L}{S + \alpha L + k} Z \tag{14}$$

The three equations for detritus follow, respectively for carbon, D_C, for nitrate, D_N, and for phosphate, D_P. The nitrogen to carbon and phosphate to carbon ratios are held constant for all picoplankton, netplankton and zooplankton sinks.

$$\left.\frac{\partial D_C}{\partial t}\right|_{source} = d_Z Z + d_S S + d_L L - k^{*}_{decC} D_C \tag{15}$$

$$\left.\frac{\partial D_N}{\partial t}\right|_{source} = R_{NC}(d_Z Z + d_S S + d_L L) - k^{*}_{decN} D_N \tag{16}$$

$$\left.\frac{\partial D_P}{\partial t}\right|_{source} = R_{PC}(d_Z Z + d_S S + d_L L) - k^{*}_{decP} D_P \tag{17}$$

The growth limitations for picoplankton and netplankton are:

$$f\,\mathrm{lim}_S = f(I) g_S(T) \frac{P}{P + k_{PS}} \Big[\frac{N}{N + k_{NS}} \boxed{e^{-\psi^{S^A}}} \leftarrow e^{-\psi_S A} \tag{18}$$

$$+ \frac{A}{A + k_{AS}}\Big]$$

$$f\,\mathrm{lim}_L = f(I) g_L(T) \frac{P}{P + k_{PL}} \Big[\frac{N}{N + k_{NL}} \boxed{e^{-\psi^{L^A}}} \leftarrow e^{-\psi_L A} \tag{19}$$

$$+ \frac{A}{A + k_{AL}}\Big]$$

where $f(I)$ is the limitation due to the incident light I:

$$f(I) = \frac{I}{I_0} e^{\left\{1 - \frac{I}{I_0}\right\}} \tag{20}$$

and g_S, g_L are the limitations due to the temperature T:

$$g_S(T) = \left(\frac{T_{S\,max} - T}{T_{S\,max} - T_S}\right)^{b_S(\boxed{T_S\,\mathrm{max}} - T_S)} e^{b_S(T - T_S)} \quad \leftarrow T_{S\,max} \tag{21}$$

$$g_L(T) = \left(\frac{T_{L\,max} - T}{T_{L\,max} - T_L}\right)^{b_L(\boxed{T_L\,\mathrm{max}} - T_L)} e^{b_L(T - T_L)} \quad \leftarrow T_{L\,max} \tag{22}$$

Parameters are reported in Table 1.

Starred parameters in the equations correspond to those in Table 1 multiplied by $\vartheta^{(T - T_0)}$.

The nominal trajectory of the model, Fig. 2, correctly reproduces the formation of the well known 'deep chlorophyll maximum'. In fact, the dynamic of the primary production is first triggered by light and temperature and therefore the model shows a bloom of diatoms in the early spring, followed by the bloom of microflagellates, which reach their maximum of productivity at higher level of light intensity and temperature. Such blooms cause a rapid depletion of nutrients, which is more pronounced near the surface, where light intensity is higher.

Grazing activity starts affecting the phytoplanktonic stocks toward the end of the spring. A local sensitivity

Table 1
List of parameters

Parameter	Definition	Unit
μ_S	Maximum growth rate of picoplankton	s^{-1}
k_{PS}	Phosphorus half-saturation of picoplankton	mg atP m^{-3}
k_{NS}	Nitrogen half-saturation of picoplankton	mg atN m^{-3}
k_{AS}	Ammonia half-saturation of picoplankton	mg atN m^{-3}
ψ_S	Ammonia inhibition coefficient for picoplankton	mg atN^{-1} m^3
μ_L	Maximum growth rate of netplankton	s^{-1}
k_{PL}	Phosphorus half-saturation of netplankton	mg atP m^{-3}
k_{NL}	Nitrogen half-saturation of netplankton	mg atN m^{-3}
k_{AL}	Ammonia half-saturation of netplankton	mg atN m^{-3}
ψ_L	Ammonia inhibition coefficient for netplankton	mg atN^{-1} m^3
k_{nit}	Nitrification rate	s^{-1}
k_{AO}	Nitrification half-saturation for oxygen	mg atO m^{-3}
R_{NC}	Nitrogen to carbon ratio	mg atN/mg atC
R_{PC}	Phosphorus to carbon ratio	mg atP/mg atC
R_{OC}	Oxygen to carbon ratio	mg atO/mg atC
R_{nit}	Nitrification oxygen	mg atO/mg atN
k_{decC}	Carbon remineralization rate	s^{-1}
k_{decN}	Nitrogen remineralization rate	s^{-1}
k_{decP}	Phosphorus remineralization rate	s^{-1}
k_{rS}	Picoplankton respiration rate	s^{-1}
k_{rL}	Netplankton respiration rate	s^{-1}
k_{exr}	Excretion rate	s^{-1}
ϵ_S	Picoplankton efficiency	
ϵ_L	Netplankton efficiency	
g	Zooplankton grazing rate	s^{-1}
α	Preference coefficient	
k	Grazing half-saturation	mg atC^{-1} m^3
d_S	Picoplankton mortality	s^{-1}
d_L	Netplankton mortality	s^{-1}
d_Z	Zooplankton mortality	s^{-1}
k_{nit}	Nitrification rate	s^{-1}
ϑ	Temperature coefficient	$°C^{-1}$
T_0	Reference temperature	°C
$T_{S\,max}$	Max. picoplankton temp.	°C
T_S	Ref. picoplankton temp.	°C
b_S	Temp. coef. for picoplankton	°C
$T_{L\,max}$	Max. netplankton temp.	°C
T_L	Ref. netplankton temp.	°C
b_L	Temp coef. for netplankton	°C
I_0	Half-saturation irradiance level	lux

analysis, based on the linearization of the trajectory of the model, has been performed on the 1-D model, indicating that many parameters, if slightly changed, have a similar influence on model output of chlorophyll and nutrients. This points out once more the uselessness of a too detailed biological description as long as experimental data are restricted to information currently available.

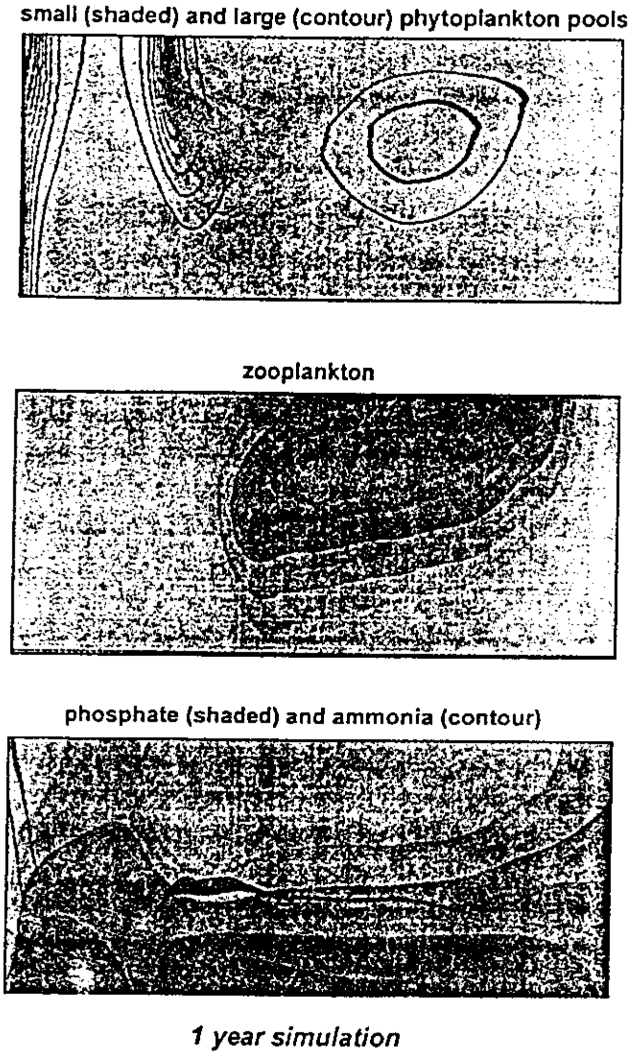

Fig. 2. 1-D time evolution (abscisses—one year of simulation) vs depth (ordinates—100 m) of picoplankton (shaded) and netplankton (contoured) concentrations, higher plate; zooplankton, middle plate; phosphate (shaded), ammonia (contour), lower plate.

4. The nitrate-based model

The nitrogen model gives the space and time evolution of inorganic nitrogen, NO_3^-, phytoplankton, PHY, zooplankton, ZOO, detritus, DET, all in nitrogen units.

The schematization of the sources for each tracer is the following

$$\left.\frac{\partial NO_3^-}{\partial t}\right|_{source} = r \cdot DET + (1-\alpha)\delta \cdot ZOO \tag{23}$$

$$- G\frac{NO_3^- \cdot PHY}{k_{NP} + NO_3^-}$$

$$\left.\frac{\partial PHY}{\partial t}\right|_{source} = G\frac{NO_3^- \cdot PHY}{k_{NP} + NO_3^-} - d \cdot PHY \tag{24}$$

$$-\gamma\frac{\mathrm{PHY}\cdot\mathrm{ZOO}}{k_{\mathrm{PZ}}+\mathrm{PHY}}$$

$$\left.\frac{\partial\mathrm{ZOO}}{\partial t}\right|_{\mathrm{source}} = \eta\gamma\frac{\mathrm{PHY}\cdot\mathrm{ZOO}}{k_{\mathrm{PZ}}+\mathrm{PHY}} - \delta\cdot\mathrm{ZOO} \qquad (25)$$

$$\left.\frac{\partial\mathrm{DET}}{\partial t}\right|_{\mathrm{source}} = d\cdot\mathrm{PHY} + (1 \qquad (26)$$

$$-\eta)\gamma\frac{\mathrm{PHY}\cdot\mathrm{ZOO}}{k_{\mathrm{PZ}}+\mathrm{PHY}} + \alpha\delta\cdot\mathrm{ZOO} - r\cdot\mathrm{DET}$$

where *d* is the respiration and mortality rate for phyto and *r* is the nutrient regeneration rate.

The limiting factor *G* for the algal growth depends on the temperature *T*, on the irradiance L_r and on the Michaelis–Menten uptake formulation. The zooplankton efficiency, η, is put to a value of 0.75, while its degradation in detritus, α, is 1/3. The zooplankton growth, γ, and mortality, δ, are chosen respectively $1.157 \times 10^{-5}\,\mathrm{s}^{-1}$ and $1.736 \times 10^{-6}\,\mathrm{s}^{-1}$; the grazing half-saturation, k_{PZ}, is 1.0 mg atN m^{-3}.

The results for the NPD aggregated description are discussed in Crispi et al. (1998) and we report only those considerations important for the discussion. The introduction of the zooplanktonic state variable gives similar results as integrated in the overall 3-D model. In fact the difference between the two submodels, i.e. with or without herbivores, is methodological: while NPD is devoted to general assessment of the trophodynamics in the overall ecosystem, NPZD is designed to estimate the bulk of biomass present in different compartments and the fluxes among them.

All the parameters are chosen in literature ranges for oligotrophic environments, after considering the sensitivity of the entire model to different values of each parameter.

This was possible because of the simplicity of the ecological model and enabled us to calibrate, considering selected results from different projects, the 3-D model to the values of detritus remineralization and sinking.

In Fig. 3 the annual mean chlorophyll concentrations, as calculated with the 3-D NPD model in Mediterranean areas deeper than 200 m, are shown. The phytoplankton biomass, averaged on the upper 20 m, is expressed in carbon units using the Redfield et al. (1963) carbon to nitrogen ratio. This field is transformed into chlorophyll concentrations using the Cloern et al. (1995) relation.

The values range from maxima values, about 1.0 mgChl m^{-3}, in the Western Mediterranean to few hundredths in the southern Ionian Sea and in the Levantine basin. Higher concentrations are visible connected with the effects of coastal upwelling along the southern and eastern Sicily coast.

In Fig. 4 the annual averages of the same quantity,

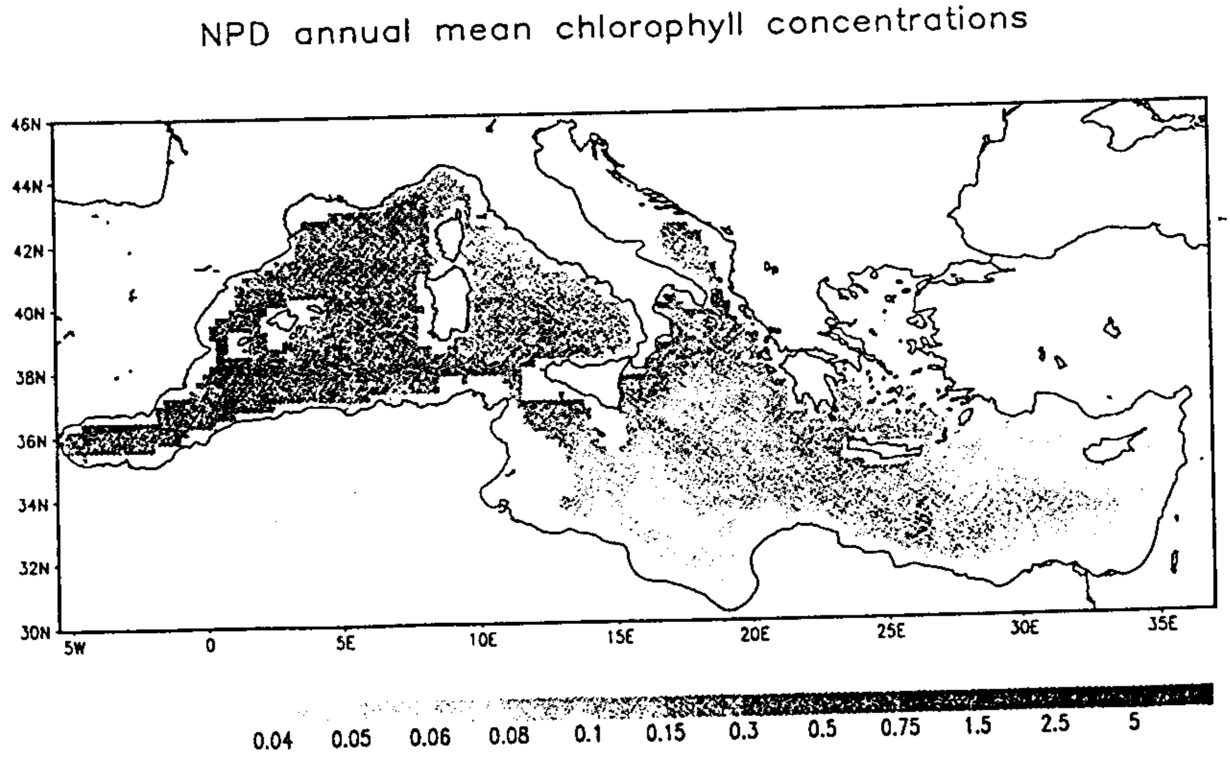

Fig. 3. Annual mean surface chlorophyll concentrations obtained from the 3-D NPD model in Mediterranean. Areas deeper than 200 m are shown (mgChl m^{-3}).

please put before units

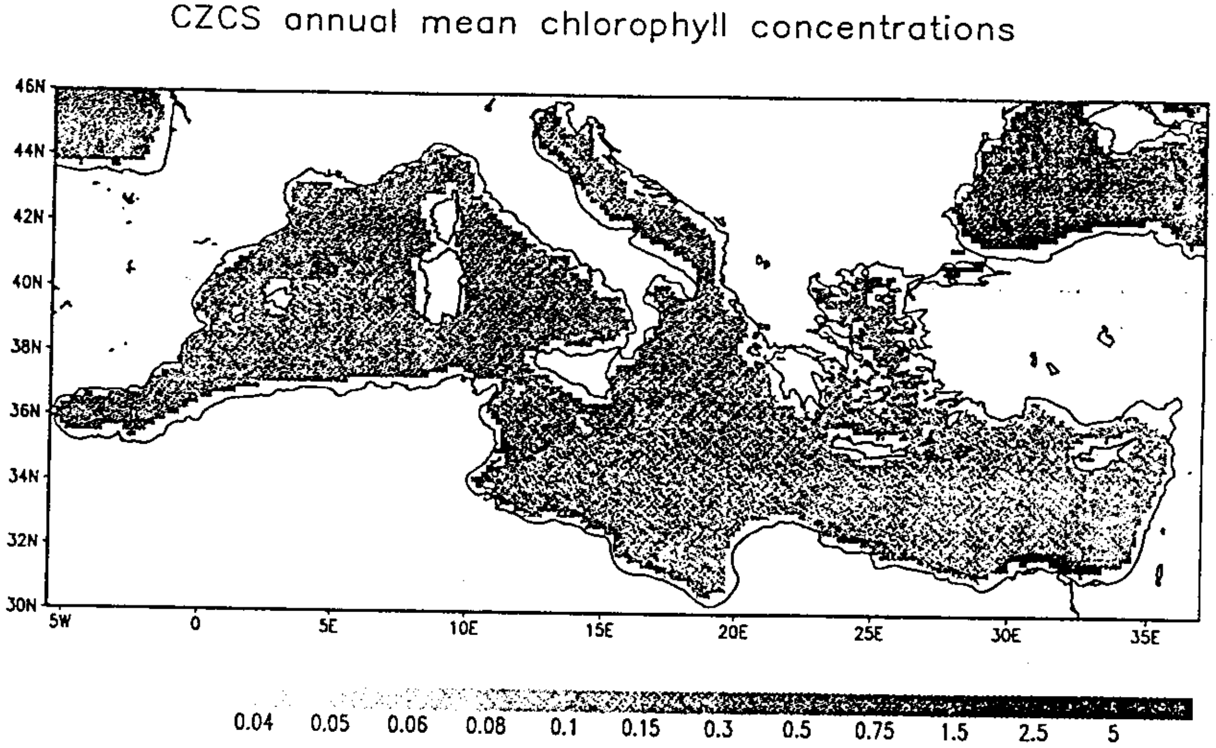

Fig. 4. Annual mean surface chlorophyll concentrations obtained after the Goddard Space Flight Center processing of the CZCS data for the years 1978–86 (mgChl m^{-3}).

this time obtained starting from the sensors of the Coastal Zone Color Scanner as analyzed by Goddard Space Flight Center, are shown.

The values are of the same order as those presented before but they are higher in the Ligurian–Provençal Sea and in some coastal areas. This similar pattern attests the relevance of the general circulation for the open ocean surface ecosystem response.

Besides its explanatory capabilities this model is able to estimate the active or passive pollutants distributions with pointwise or distributed sources for analysis of scenarios. The model is set up for integration of NPZD and of the corresponding equations tracing an active tracer, for example marked nitrogen.

Acknowledgements

This work was partially funded by the EC contract MAss Transfer and Ecosystem Response: MAS3-CT96-0051. We thank J. Baretta, R. Mosetti and J.I. Allen for helpful discussions during the meetings organized in the frame of the above-mentioned project.

References

Bisset, W.P., Meyers, M.B., Walsh, J.J., Müller-Karger, F.E., 1994. The effects of temporal variability of mixed layer depth on primary productivity around Bermuda. Journal of Geophysics Research 99 (C4). 7539–7553.

Cloern, J.E., Grenz, C., Vidergas-Lucas, L., 1995. An empirical model of the phytoplankton chlorophyll:carbon ratio—the conversion factor between productivity and growth rate. Limnology and Oceanography 40 (7). 1313–1321.

Conkright, M.E., Levitus, S., Boyer, T.P., 1994. World Ocean Atlas. 1994. Vol. 1. US Department of Commerce.

Coste, B., Gostan, J., Minas, H.J., 1972. Influence des conditions hivernales sur les productions phyto- et zooplanctoniques en Méditerranée nord-occidentale. I. structures hydrologiques et distribution des sels nutritifs. Marine Biology 16. 320–348.

Coste, B., Le Corre, P., Minas, H.J., 1988. Re-evaluation of the nutrient exchanges in the Strait of Gibraltar. Deep-Sea Research 35, 767–775.

Crise, A., Crispi, G., Mauri, E., 1998. A seasonal three-dimensional study of the nitrogen cycle in the Mediterranean Sea. Part I. model implementation and numerical results. Journal of Marine Systems (in press).

2

Crispi, G., Crise, A., Mauri, E., 1998. A seasonal three-dimensional study of the nitrogen cycle in the Mediterranean Sea. Part II. verification of the energy constrained trophic model. Journal of Marine Systems (in press).

Cruzado, A., 1995. Nutrient distributions in the Gulf of Lions (northwestern Mediterranean) during cruise RRV DISCOVERY (July 1993). In: Matrun, J.-M., Barth, H. (Eds), EROS 2000 (European River Ocean System) Fifth Workshop on the North-West Mediterranean Sea Hamburg (Germany) 28–30 March 1994, EUR 16130, pp. 69–77. MARTI

Dugdale, R.C., Wilkerson, F.P., 1988. Nutrient sources and primary production in the Eastern Mediterranean. Oceanologia Acta 9, 179–184.

Eppley, R.W., Peterson, B.J., 1979. Particulate organic matter flux and planktonic new production in the deep ocean. Nature 282, 677–680.

Fasham, M.J.R., Duklow, H.W., McKelvie, S.M., 1990. A nitrogen-based model of plankton dynamics in the oceanic mixed layer. Journal of Marine Research 48, 591–639.

Holling, C.S., 1965. The functional response of predators to prey density. Memoranda of the Entomological Society of Canada 45, 5–60.

Lassiter, R.R., Kearns, D.K., 1974. Phytoplankton population changes and nutrient fluctuations in a simple aquatic ecosystem model. In: Middlebrookes, E.J., Falkenberg D.H., Maloney, T.E. (Eds), Modeling the Eutrophication Process. Ann Arbor Science, pp. 131–138.

Levitus, S., Conkright, M.E., Reid, J.L., Najjar, R., Mantyla, A., 1993. Distribution of nitrate, phosphate and silicate in the world ocean. Progress in Oceanography 31, 245–273.

Margalef, R., 1985. Environmental control of the mesoscale distribution of primary producers and its bearing to primary production in the Western Mediterranean. In: Moraitou-Apostolopoulou, M., Kiortsis, V. (Eds), Mediterranean Marine Ecosystems. Plenum Press, New York, pp. 213–229.

Michaels, A.S., Silver, M.W., 1988. Primary production, sinking fluxes and the microbial food web. Deep-Sea Research 35 (4), 473–490.

Rabitti, S., Civitarese, G., Ribera, M., 1994. Data Report cruise POEM-BC—October 1991—Ionian Basin and Sicily Channel. Part II: chemical and biological data. Tech. Rep. No. 13/94-CNR/IBM.

Redfield, A.C., Ketchum, B.H., Richards, F.A., 1963. The Influence of Sea Water. In: Hill, M.N. (Ed.), The Sea, vol. 2. Interscience, New York, pp. 26–77.

Steele, J.H., 1962. Environmental control of photosynthesis in the sea. Limnology and Oceanography 7, 137–150.

Zavatarelli, M., Raicich, F., Bregant, D., Russo, A., Artegiani, A., 1998. Climatological Biogeochemical Characteristics of the Adriatic Sea. Journal of Marine Systems (in press).

Query No. 5

Query No. 6